ISBN: 978-3-95450-248-6 ISSN: 2673-5490 doi: 10.18429/JACoW-IPAC25-TUPB007

RADIATION LEVELS FROM A BEAM GAS CURTAIN INSTRUMENT AT THE LHC AT CERN DURING ION OPERATION

D. Prelipcean, G. Lerner, R. García Alía, G. Schneider, D. Butti,
O. Sedlacek, R. Veness, C. Castro Sequeiro, M. Ady
CERN, Geneva, Switzerland

Abstract

A prototype Beam Gas Curtain (BGC) monitor was installed on beam 1 at the Large Hadron Collider (LHC) at CERN to investigate its potential for providing 2D images of the transverse beam profile during the ongoing LHC Run 3 (2022 - to date) operation and in view of the High Luminosity LHC upgrade (HL-LHC). By design, the BGC operation generates collisions between the beam particles and an injected gas jet, proportionally to the beam intensity and the gas density, possibly causing radiation-induced issues to the downstream accelerator equipment. This operation has been studied for the proton run, and now the scenario for lead (Pb^{82+}) ion beam is scrutinized. The radiation showers from the BGC are characterized using measured data from different LHC radiation monitors during the Run 3 BGC operation, along with Monte Carlo simulations with the FLUKA code.

INTRODUCTION

The scope of this paper is to analyse the radiation levels induced by the Beam Gas Curtain (BGC) [1, 2] monitor installed in Interaction Region 4 (IR4) of the Large Hadron Collider (LHC) at CERN [3] in the context of the Radiation to Electronics (R2E) effort [4]. Similar work has been carried out to study the radiation levels generated by the operation of the BGC during proton operation [5], as well as for the Beam Gas Vertex (BGV) [6, 7] instrument; the BGV will finally not be part of the HL-LHC baseline, but rather replaced by the Beam Gas Ionisation (BGI) [8, 9] instrument in operation. The radiation levels measured by the Beam Loss Monitors (BLMs) [10] during the LHC Run 3 (2022 - to date) for the lead (Pb^{82+}) ion beam operation (lasting for about 1 month/year) are compared with dedicated FLUKA [11–13] simulations, as well as to the proton operation.

RADIATION SOURCE

At the BGC, the intentional injection of gas (Neon) increases the local gas density used for the 2D beam image reconstruction [1]. This leads as well to radiation showers and thereby higher radiation levels in the tunnel (relevant for equipment and electronics) and heat loads on magnets (for quench protection). The radiation level rates dR/dt are assumed to be proportional to the interaction rate of inelastic beam-gas collisions:

$$\frac{dR}{dt} \propto N(t) \cdot f \cdot \sigma \cdot \Theta(t; s_a, s_b) \tag{1}$$

which is proportional to the beam intensity $N(t)$, the LHC revolution frequency $f = 11245$ Hz, the interaction cross section σ_{Pb+Ne} for an Pb ion beam of E =2.76 TeV/n (with a PbPb center of mass energy $\sqrt{s}$ =5.52 TeV/n) hitting the Neon gas atoms, and the integrated gas density profile $\Theta(t; s_a, s_b)$ along the s-coordinate in the accelerator region $[s_a, s_b]$.

The gas density profile used for the BGC demonstrator in FLUKA [12, 13] has been simulated using the MOLFLOW+ [14] package; a more detailed description about how these profiles are obtained can be found in ref. [15]. The gas curtain used to generate the signal for the BGC amounts to about 20% of the total integrated gas density $\Theta(s_a, s, b)$. The remaining tails of the gas distribution constitutes background is an unavoidable byproduct of the gas injection and is limited by the pumping capacity of the vacuum system surrounding the instrument.

There are two main differences during ion operation compared to the proton operation [5]. Firstly, the beam intensity is lower, for ions at $N_t^{Pb} = 8 \cdot 10^{13}$ charges per beam (against $N_t^p = 3 \cdot 10^{14}$ per beam for protons). Secondly, if for the proton case the only relevant physical process leading to local radiation levels was the inelastic interaction, for the case of ions there is an additional electromagnetic dissociation component. The interaction cross section scales with the "surface" of the target nucleus as seen by the beam $\sigma_{inel}^{Pb+Ne} = \sigma_{inel}^{pp} \cdot \left(A_{Pb}^{1/3} + A_{Ne}^{1/3}\right)^2$ [16]. The FLUKA estimate for this is σ_{inel}^{Pb+Ne}=3800 mb, about 10 times larger than the σ_{inel}^{p+Ne} case [7].

FLUKA SIMULATION

The FLUKA Monte Carlo code is capable of simulating the radiation shower caused by the beam-gas interactions. The position of the interactions is sampled along a Continuous Distribution Function (CDF) given by the gas density profile in the beam pipe, and the interaction secondaries are propagated in the geometry model of the LHC tunnel. Figure 1 displays a top view of the Total Ionizing Dose (TID) at beam height due to the radiation shower caused by the beam-gas collisions, which extends longitudinally over several tens of meters. In addition to the TID, the FLUKA simulation can be used to compute different radiation level quantities in the tunnel that are relevant for R2E applications and beyond, as well as energy deposition and heat loads in the inner layers of the exposed magnets.

ISBN: 978-3-95450-248-6 ISSN: 2673-5490 doi: 10.18429/JACoW-IPAC25-TUPB007

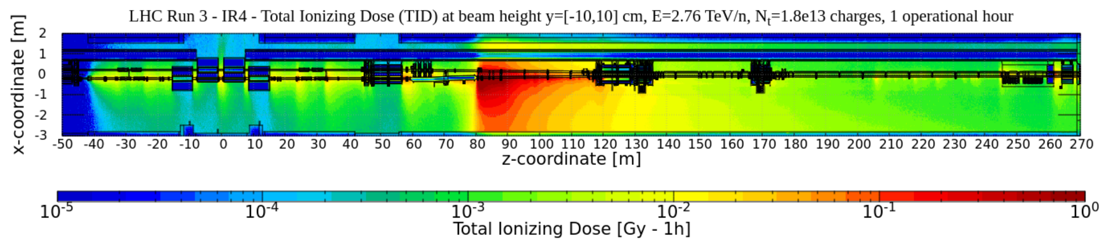

Figure 1: FLUKA simulated radiation shower caused only by the BGC demonstrator (z=–42 m) on beam 1 (beam direction: from left to right) for LHC operation, as ZX view, displaying how the shower extends several hundreds of meters. The TID is provided at beam height, for a beam at E =2.76 TeV/n with a nominal intensity of $N_t = 8 \cdot 10^{13}$ charges per beam, and normalized to 1 BGC operational hour.

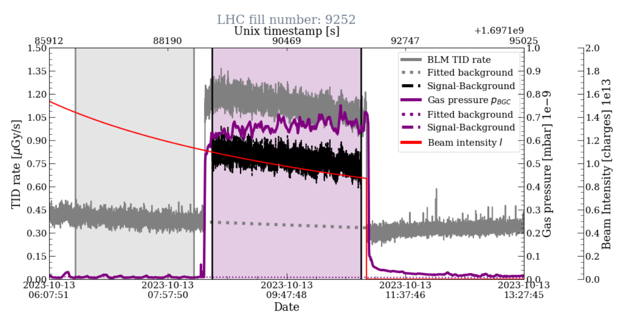

Figure 2: The measured TID rate for the most exposed BLM (z=75 m) downstream of the BGC during a reference LHC fill (here, #9252), plotted alongside the beam 1 intensity N_p and the BGC pressure gauge reading p_{BGC}. Both the BLM TID rate and the pressure gauge measurements have been fitted with background models, either exponentially decaying (following the beam intensity evolution) or a constant.

MEASURED RADIATION LEVELS

The primary goal of the analysis on measured data was to verify the proportionality between the radiation levels rate as measured by the available radiation monitors (explained below) and the product of beam intensity and gas pressure, based on Eq. (1). The considered data set consists of the TID measurements by the BLMs. They are (mostly) Ionization Chambers placed along the accelerator that detect particle showers caused by the beam losses in their active volume of N_2 gas. The BLMs are capable of measuring dose rates with good time resolution down to integration intervals of 40 µs (here, the 1 s running sum has been used). Figure 2 showcases that when gas is injected in the BGC, the BLM TID rate signal increases proportionally to the product of pressure and intensity. However, the background TID levels are not negligible, leading to the need of background modelling (exponentially decaying behaviour over time, following the beam intensity) and subtraction procedures.

Similar as for the proton analysis [5], one can plot the background subtracted TID normalized by the total number of passing charges as measured by the Beam Current Transformers (BCT) instruments [17] against the background subtracted BGC pressure gauge reading, shown in Fig. 3. The

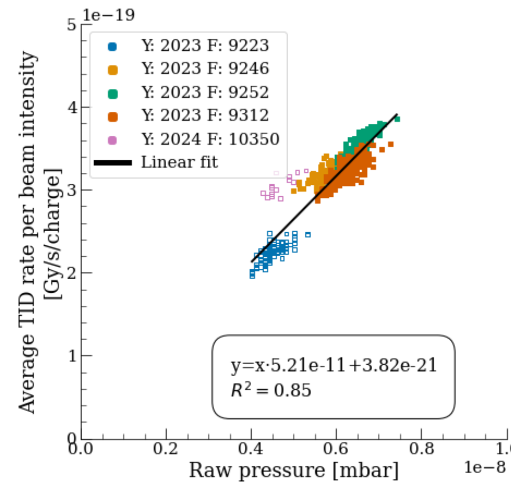

Figure 3: The measured TID of the most exposed BLM (z=75 m) divided by the beam intensity N_p, plotted against the average BGC pressure gauge reading p_{BGC}, for each timestamp of the pressure gauge measurements (1 s) time resolution), for 5 fills during Run 3 operation.

radiation levels downstream of the instrument correlate well with the beam intensity and the gas pressure, indicating that the BGC is indeed the main source of prompt radiation for this BLM. For each monitor downstream of the instrument, the same procedure is repeated, and visible correlations (considered as $R^2 > 0.3$) between the TID per unit intensity and the gauge pressure are observed up to 200 m downstream of the BGC.

LHC BGC DEMONSTRATOR BENCHMARK AND COMPARISON WITH PROTON RUN

The radiation levels simulated by FLUKA are compared to the BLM measurements (background-subtracted) taken during the operation of the BGC demonstrator in Run 3 (2022-to date) in Fig. 4. The shape of the BLM TID profile is well reproduced with a good global agreement within at least a factor of 2 between simulations and measurements,

ISBN: 978-3-95450-248-6 ISSN: 2673-5490 doi: 10.18429/JACoW-IPAC25-TUPB007

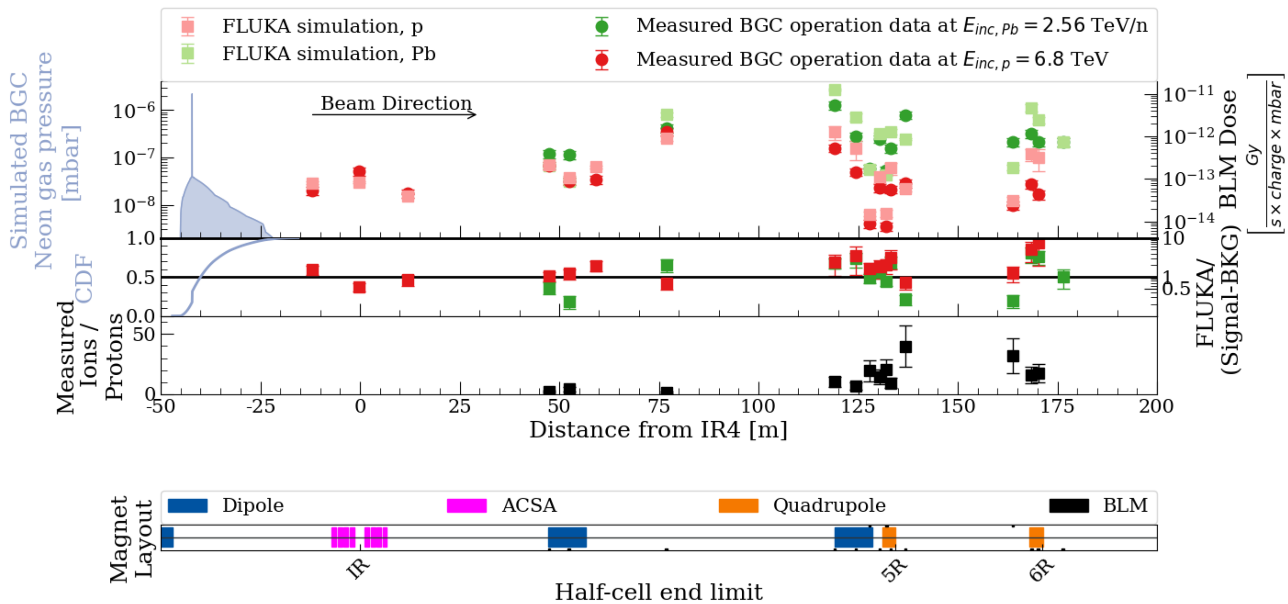

Figure 4: Top panel: (Left axis) The BGC gas density profile used to generate the radiation shower, together with the (right axis) BLM data downstream the BGC placed on beam 1 as measured over the LHC Run 3 proton operation (red points) and ion operation (green points), as well as those simulated by FLUKA. Mid panel: (Left axis) The CDF computed from the gas profile, together with the (right axis) ratio between the simulated values over background (BKG) subtracted measured data for Run 3, for both protons (red) and ions (green). Bottom panel: The ratio of measured radiation levels rates (normalized to unit charge and pressure) of the ion over proton operation. Bottom pad: The machine layout and the BLM locations for the LHC machine.

with some outliers at large distance from the radiation source. Since the simulation tends to overestimate the radiation levels with the distance from the radiation source, the main source of discrepancy is assumed to be geometry mismodelling due to approximations, in particular lack of implemented material budget, which could be further improved upon. In other areas of the LHC, such benchmarks have achieved similar levels of agreement [18–20].

The radiation levels from ion operation are also compared to those from the proton operation in Fig. 4. The BLM TID rates for the ion operation, normalized per unit charge (with Pb^{82+} ion beam) and unit pressure, reveal a different pattern, with a larger fraction of the radiation further away from the BGC instrument. The first three BLMs do not have any measured data, as the measured BGC-driven losses are undistinguishable from background in this area. The lower pad of Fig. 4 indicates that the ratio of normalized ion radiation levels to proton radiation levels can reach locally a factor of a few tens. However, when taking into consideration the beam intensity, the absolute radiation level rates are comparable. Cumulatively, as ion operation typically lasts for about 1 month, compared to the high beam intensity proton operation for about 6 months, the integrated radiation levels at IR4 are largely dominated by the proton run, and not by the ion run.

CONCLUSIONS

This study presents the assessment of the radiation environment generated by the BGC instrument during heavy ion operation at the LHC. Beyond confirming the proportionality between measured radiation levels and beam-gas interaction parameters, the results establish the BGC as a well-characterized and localized source of radiation that can be robustly predicted with modern simulation tools such as FLUKA. The benchmarking effort not only confirms the validity of the simulation chain but also demonstrates that the radiation footprint from the BGC extends beyond the immediate vicinity of the instrument—up to more than 200 m downstream - thus highlighting the long-range impact of localized sources in a high-energy hadron collider environment. From an operational perspective, this work consolidates confidence in safely integrating active gas-based beam profile monitors within the LHC, particularly relevant in view of the increasing demands on diagnostics precision in the HL-LHC era, and beyond.

ACKNOWLEDGEMENTS

This work has been partly sponsored by the Wolfgang Gentner Programme of the German Federal Ministry of Education and Research (grant no. 13E18CHA). Research supported by the HL-LHC project.

ISBN: 978-3-95450-248-6 ISSN: 2673-5490 doi: 10.18429/JACoW-IPAC25-TUPB007

REFERENCES

[1] H. D. Zhang, A. Salehilashkajani, O. Sedlacek, and C. P. Welsch, "Characterization of a supersonic molecular beam for charged particle beam profile monitor", *Vacuum*, vol. 208, p. 111701, 2023. doi:10.1016/j.vacuum.2022.111701

[2] A. Salehilashkajani *et al.*, "A gas curtain beam profile monitor using beam induced fluorescence for high intensity charged particle beams", *Applied Physics Letters*, vol. 120, no. 17, p. 174101, Apr. 2022. doi:10.1063/5.0085491

[3] O. S. Brüning *et al.*, "LHC Design Report, Vol. I: The LHC Main Ring", CERN, Geneva, Rep. CERN-2004-003-V-1, 2004. doi:10.5170/CERN-2004-003-V-1

[4] Radiation to Electronics (R2E) at CERN. https://r2e.web.cern.ch/

[5] D. Prelipcean *et al.*, "Radiation levels from a Beam Gas Curtain instrument at the LHC at CERN", in *Proc. IPAC'24*, Nashville, TN, pp. 3393–3396, 2024. doi:10.18429/JACoW-IPAC2024-THPG58

[6] A. Alexopoulos *et al.*, "Noninvasive LHC transverse beam size measurement using inelastic beam-gas interactions", *Phys. Rev. Accel. Beams*, vol. 22, no. 4, p. 042801, 2019. doi:10.1103/PhysRevAccelBeams.22.042801

[7] D. Prelipcean *et al.*, "Radiation levels produced by the operation of the Beam Gas Vertex monitor in the LHC tunnel at IR4", in *Proc. IPAC'23*, Venice, Italy, pp. 4629–4632, May 2023. doi:10.18429/JACoW-IPAC2023-THPL082

[8] S. Levasseur *et al.*, "Development of a rest gas ionisation profile monitor for the CERN Proton Synchrotron based on a Timepix3 pixel detector", *J. Instrum.*, vol. 12, no. 02, p. C02050, Feb. 2017. doi:10.1088/1748-0221/12/02/C02050

[9] H. Sandberg, "Development of a Novel Transverse Beam Profile and Emittance Monitor for the CERN Proton Synchrotron", Ph.D. thesis, University of Manchester, UK, 2020. https://cds.cern.ch/record/2747870

[10] E. B. Holzer *et al.*, "Beam Loss Monitoring System for the LHC", *IEEE Nucl. Sci. Symp.*, vol. 2, pp. 1052–1056, Oct. 2005. doi:10.1109/NSSMIC.2005.1596433

[11] FLUKA website. https://fluka.cern

[12] FLUKA.CERN Collaboration, "New Capabilities of the FLUKA Multi-Purpose Code", *Front. Phys.*, vol. 9, 2022. doi:10.3389/fphy.2021.788253

[13] FLUKA.CERN Collaboration, "Overview of the FLUKA code", *Ann. Nucl. Energy*, vol. 82, pp. 10–18, 2015. doi:10.1016/j.anucene.2014.11.007

[14] R. Kersevan and M. Ady, "Recent Developments of Monte-Carlo Codes Molflow+ and Synrad+", in *Proc. IPAC'19*, Melbourne, Australia, May 2019, pp. 1327–1330. doi:10.18429/JACoW-IPAC2019-TUPMP037

[15] C. Castro Sequeiro *et al.*, "Beam gas curtain monitor: vacuum studies for lhc integration and operation", *Phys. Rev. Accel. Beams*, vol. 27, no. 4, p. 043201, Apr. 2024. doi:10.1103/PhysRevAccelBeams.27.043201

[16] M. Ferro-Luzzi, "Beam-gas interactions", *arXiv*, 2020. doi:10.48550/ARXIV.2006.06490

[17] R. Jones *et al.*, "Introduction to beam instrumentation and diagnostics", CERN, Geneva, Switzerland, Rep. CERN-2014-009, 2014. doi:10.5170/CERN-2014-009.23

[18] A. Lechner *et al.*, "Validation of energy deposition simulations for proton and heavy ion losses in the cern large hadron collider", *Phys. Rev. Accel. Beams*, vol. 22, no. 7, Jul. 2019. doi:10.1103/PhysRevAccelBeams.22.071003

[19] D. Prelipcean *et al.*, "Comparison Between Run 2 TID Measurements and FLUKA Simulations in the CERN LHC Tunnel of the ATLAS Insertion Region", in *Proc. IPAC'22*, Bangkok, Thailand, Jun. 2022, pp. 732–735. doi:10.18429/JACoW-IPAC2022-MOPOMS042

[20] D. Prelipcean *et al.*, "Comparison between Run 2 SEU measurements and FLUKA simulations in the CERN LHC tunnel and shielded alcoves around IP1/5", in *Proc. IPAC'23*, Venice, Italy, pp. 4633–4636, May 2023. doi:10.18429/JACoW-IPAC2023-THPL083